Stretching fields and mixing near the transition to non-periodic two-dimensional flow

M. J. Twardos,[1] P. E. Arratia,[2,3] M. K. Rivera,[1] G. A. Voth,[4] J. P. Gollub,[3] and R. E. Ecke[1]

[1] *Condensed Matter & Thermal Physics Group and The Center for Nonlinear Studies, Los Alamos National Laboratory, Los Alamos, New Mexico 87545*
[2] *Physics Department, University of Pennsylvania, Philadelphia, PA 19104*
[3] *Physics Department, Haverford College, Haverford, PA 19041*
[4] *Physics Department, Wesleyan University, Middletown, CT 06459*

(Dated: November 30, 2007)

Although time-periodic fluid flows sometimes produce mixing via Lagrangian chaos,the additional contribution to mixing caused by non-periodicity has not been quantified experimentally. Here, we do so for a quasi two-dimensional flow generated by electromagnetic forcing. Several distinct measures of mixing are found to vary continuously with Reynolds number, with no evident change in magnitude or slope at the onset of non-periodicity. Furthermore, the scaled probability distributions of the mean Lyapunov exponent have the same form in the periodic and non-periodic flow states.

PACS numbers: 47.52.+j, 05.45.-a, 47.20.Ky

Fluid mixing, often aided by turbulent fluctuations, is intimately connected with the transport of mass or energy. Understanding and characterizing mixing is crucial to applications of scientific and technological importance, ranging from the redistribution of heat in the atmosphere and oceans to the efficient combustion of air-fuel mixtures. While turbulent flows generally produce strong mixing, it is also well known that time-periodic flows, even in two-dimesions, can also mix by Lagrangian chaos or chaotic advection [1–3] which causes nearby fluid elements to separate exponentially in time. Although there have been many studies of mixing in both periodic and turbulent flows, a quantitative experimental comparison of mixing properties in periodic and non-periodic regimes for the same system is lacking.

One way to do this is to measure stretching fields [4, 5] which provide the local deformation of an infinitesimal circular fluid element over a finite time interval Δt. The logarithm of the stretching (after first dividing by Δt) gives the finite-time Lyapunov exponent $\langle\lambda\rangle$ for separation of nearby fluid elements at each point in a flow. For periodic two-dimensional flows, stretching fields have been shown to be closely related to the mixing of a passive scalar concentration field [6–8] . An equivalent of stretching fields was first calculated numerically for a non-periodic model system by Varosi et al. [9]. Mixing in tidal currents were also analyzed using similar dynamical systems methods [10]. Until recently [11], however, the extension of these ideas to systems that are non-periodic or weakly turbulent has been possible only in numerical simulations [4].

Previous investigations of turbulent flows have considered passive scalar dynamics [12, 13] and Lagrangian dispersion of particle clusters [14]. Lagrangian reference frame measurements such as single particle dynamics [15], the separation of particle pairs [16, 17], and the deformation of particle clusters [18] provide additional insight into the deformation of fluid elements associated with turbulence. Recently, stretching fields were obtained [11] in a rotating turbulent three dimensional flow, where the rotation imposes a quasi-two-dimensional constraint. Finite-time Lyapunov exponents were also measured experimentally for elastic turbulence in a complex fluid [19] but the mechanisms for chaotic dynamics in this very low Re system may be quite different from more traditional fluid turbulence. Although these results show promise for the general applicability of this technique to more complex flows, experimental determination of Lyapunov exponents as a function of Reynolds number, Re, for turbulent flows has not been reported.

In the research reported here, we investigate mixing in a conducting stratified fluid driven by a temporally-periodic electric current in the presence of a spatially-random array of magnets. We demonstrate using stretching field analysis that the mean finite-time Lyapunov exponent $\langle\lambda\rangle$ is proportional to the root-mean-square (rms) rate of strain σ_{rms} and the exponential decay rate α of the number of particles in a small region, as Re varies. As the flow changes from periodic to non-periodic with increasing Re, we find that the probability distribution function (PDF) collapses to a universal curve and $\langle\lambda\rangle$ increases smoothly without any discontinuity or change in slope at the transition .

The experimental setup, described in detail elsewhere [20], consists of a 3 mm conductive layer of saturated salt water over a random magnet array with two graphite electrodes at opposing ends and a mean magnet spacing of $L_m = 2$ cm. Between the salt water and the magnet array is a 3 mm layer of Fluorinert, which is a dielectric, immiscible fluid with a density larger than water and a viscosity about 70% that of water. Fluorinert acts as a buffer layer and reduces drag on the upper conductive layer. A sinusoidal controlled voltage with a frequency of 0.1 Hz (or a period $T = 10$ s) is applied across the graphite electrodes. The resultant current in the presence of the magnets produces a Lorentz

force that drives the fluid layer periodically, producing a periodic or non-periodic (weakly turbulent) response depending on the voltage. The root-mean-square (rms) speed, strain and vorticity of the fluid, u_{rms}, σ_{rms} and ω_{rms}, respectively, are adjusted by changing the driving voltage.

The fluid is seeded with tracer particles with a diameter of approximately 100 μm, evenly distributed over the cell area of 15 × 15 cm^2. The system is illuminated with flashlamps synchronized with a high speed camera. The frame rate of the camera varies between 10 and 60 Hz depending on u_{rms}. The camera, with resolution 1024 by 1280 pixels, captures motion for about 10 forcing periods in a centered region of the flow with dimensions 10 cm × 13 cm. High resolution velocity fields are obtained using a particle tracking algorithm that identifies and tracks roughly 40,000 particles per image pair.

The experiment is performed for different drive voltages that produce a range of Reynolds numbers Re, defined as $Re \equiv u_{rms}^2/\nu\omega_{rms}$ where $\nu \approx 0.01$ cm^2/s is the kinematic viscosity of water. Values of Re range between 5 and 110. Non-periodicity is measured by determining the velocity correlation coefficient $F(T) = \langle u(t)u(t+T)\rangle/\langle u^2\rangle$, where the average is taken over space and time and T is the forcing period. The value of $F(T)$ is unity for the lowest Re and decreases to 0.25 for the highest Re. The transition to weakly turbulent flow occurs around $Re = 35$ where $F(T)$ begins to deviate slightly from one. Values of u_{rms} vary between 0.14 cm/s and 1.63 cm/s and increase monotonically with driving voltage and Re. The values of σ_{rms} and ω_{rms} are about the same for these experiments, and both increase with the driving voltage. Over the whole Re range, most of the energy in the velocity power spectrum E(k) is contained in the range $k/2\pi < 0.5$ cm^{-1}; this corresponds to the characteristic injection scale (magnet spacing) of about 2 cm. Below this characteristic scale, the spectrum is almost independent of k without any appreciable indication of an inverse energy cascade region, whereas the spectrum decreases rapidly at higher k with E(k) $\sim k^{-4}$.

Stretching is a fundamental measure of the mixing of fluid elements in which deformations of virtual fluid elements advected by the velocity field are measured over a time interval, or map length, Δt [2, 4, 5]. We compute Lagrangian trajectories using a virtual particle tracking algorithm that measures future (or past) particle positions. The Lagrangian trajectories determine a flow map Φ, which contains information about the future positions of particles that began at a given point (x, y). Deformations are measured by determining the right Cauchy Green strain tensor

$$C_{ij} = \sum_{k=1,2} \left(\frac{\partial \Phi_k}{\partial x_i}\right)\left(\frac{\partial \Phi_k}{\partial x_j}\right), \qquad (1)$$

where the derivatives are evaluated using a center-difference scheme and the trajectories are rescaled every 5 frames (0.25 s) to maintain the area preserving character of the deformation.

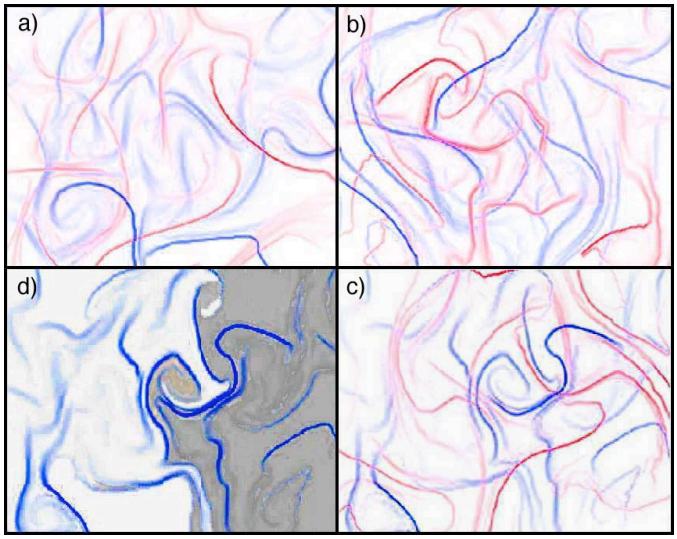

FIG. 1: (Color Online) Stretching fields (see text) at constant phase of the forcing (negative going zero crossing) with red and blue indicating forward and backward in time fields, respectively: a) periodic flow ($Re = 7.8$) with a map interval $\Delta t = 10$ s; b) weakly turbulent or non-periodic flow ($Re = 108$) with $\Delta t = 1$ s; c) same as in b) but one forcing period later (10 s); d) reverse stretching field for the case shown in b) with virtual dye placed in the flow and advected by the velocity fields to demonstrate that passive impurities do not cross lines of large past stretching.

The stretching for each trajectory, either forward or backward in time, $S(x_0, y_0)$, where (x_0, y_0) denotes the initial particle position, is determined by calculating the square root of the maximum eigenvalue of C_{ij} at each point. We start with particles on a regular grid with resolution 256 × 256 corresponding to spacing of 0.05 cm. In Fig. 1a, we show stretching fields for a periodic flow with $Re = 7.5$, with red (or blue) indicating the intensity of stretching for mappings going forward (or backward) in time. The mapping interval is taken to be one forcing period, $\Delta t = 10s$. The sharp structures, already noted in previous work [6], indicate regions of strong stretching over Δt. For comparison, we show in Fig. 1b the stretching field for weakly turbulent (non-periodic) flow with $Re = 108$. Because u_{rms} is much larger in the latter case, we choose $\Delta t = 1s$ so that the net displacements are roughly equal, in order to compare the two fields.

The stretching fields in Figs. 1a,b are qualitatively similar: both exhibit a moderate density of sharp lines associated with large stretching. On the other hand, the stretching field of the weakly turbulent case does not repeat. For example, one forcing period later the stretching field of the periodic flow shown in Fig. 1a is the same (not shown). For the non-periodic flow shown in Fig. 1b, however, the stretching field is very different one period later,

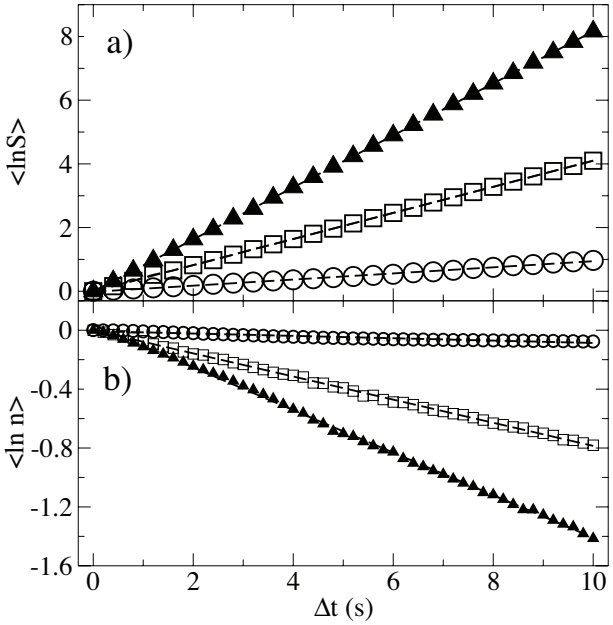

FIG. 2: a) Logarithm of stretching $\langle \ln S \rangle$ vs time increment Δt for periodic (Re=7.8, ◯) and turbulent (Re=64, □ and Re=108, ▲) flows; the growth is exponential with dashed line fits to the curves yielding the Lyapunov exponent. b) Areal particle density n(Δt) vs Δt showing dispersion of particles seeded uniformly over a box of size L=6 cm, for different Re: 7.8 (◯), 32 (□), and 108 (▲). The decay, averaged over space and over several phases of the forcing, is exponential and yields a normalized decay constant α indicated by the dashed line fits to each curve.

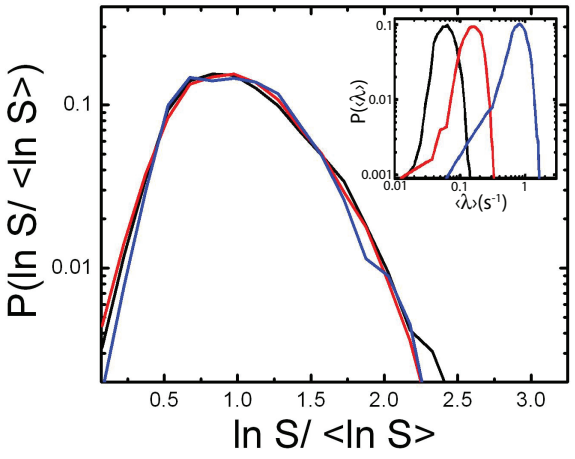

FIG. 3: (Color Online) Probability distribution of the normalized stretching ln $S/\langle \ln S \rangle$ for Re: 7.5 (black), 32(red), 108 (blue). The inset shows the PDFs of $\langle \lambda \rangle = \ln S/\Delta t$ for the same Re as in a). The statistics are not significantly affected by the transition to non-periodic flow.

as shown in Fig. 1c.

For periodic flow, dye concentration contours are observed to align with the reverse stretching fields lines [6, 7], i.e., dye and other passive scalars introduced into the flow do not cross the lines of large past stretching [6]. It has been proposed that stretching field ridges in weakly turbulent flow may play a similar role [11]. We test this hypothesis by observing the mixing of virtual dye in the turbulent case and observing the alignment of the dye with the reverse stretching field. As can be seen in Fig. 1d, the impurity does not cross lines of large past stretching, which serve as barriers to transport as in the periodic case.

Stretching fields provide a quantitative measure of mixing via evaluation of the mean stretching or the average finite-time Lyapunov exponent $\langle \lambda \rangle$. From experimental stretching fields such as those shown in Figs. 1a-c, we compute the stretching S for each point on the grid and average $\ln S$ over the full field. As in any calculation of Lyapunov exponents [21], small displacements are necessary to measure exponential growth accurately. Thus, we rescale the particle separations in the cluster (a central point and 4 nearest-neighbor points) every fifth frame (about 0.1 s) to keep them sufficiently small. A mean Lyapunov exponent $\langle \lambda \rangle$ of each field is obtained as the slope of $\langle \ln S \rangle$ versus Δt as illustrated in Fig. 2a for a periodic state with $Re = 7.8$ and for turbulent states with $Re = 64$ and $Re = 108$, respectively. The straight line demonstrates the exponential growth behavior expected in the measurement of $\langle \lambda \rangle \equiv \langle \ln S \rangle / \Delta t$.

To augment our characterization of mixing, we consider another measure of the mixing properties of the flow: the rate at which particles leave a fixed area [22, 23]. This rate is closely related to Taylor dispersion of individual particles [24]. We measure the dispersion of a uniform seeding of particles in an area L=6 cm on a side (averaged over an ensemble of areas chosen from the entire digitized image), and find that the areal density of particles $n(\Delta t)$ decreases in time with an exponential dependence and a characteristic rate α, as shown in Fig. 2b. In our implementation of this method, once a particle leaves the box, it is discarded.

In addition to average quantities, we also consider the normalized PDFs of ln $S/\langle \ln S \rangle$, averaged over all the frames in each data set, as shown in Fig. 3 (unnormalized PDFs of $\langle \lambda \rangle$ are shown in the inset). Included are several data sets corresponding to a range of Re values spanning the interval that includes both periodic and weakly turbulent (non-periodic) flow states. The excellent collapse to a non-Gaussian PDF demonstrates that there is no significant change in statistics as Re increases from the periodic to the non-periodic or weakly turbulent range.

In Fig. 4a, we show that the mean Lyapunov exponent, $\langle \lambda \rangle$, the rate of strain, normalized (arbitrarily) by a factor of 3 $\sigma = \sigma_{rms}/3$ for comparison with $\langle \lambda \rangle$), and the areal particle density decay rate α are proportional

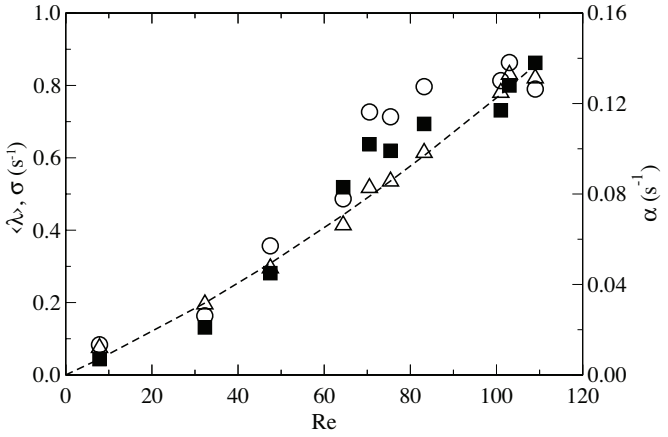

FIG. 4: The average Lyapunov exponent $\langle\lambda\rangle$ (△), the normalized (for comparison) rate of strain $\sigma = \sigma_{rms}/3$ (◯), and the areal particle density decay rate α (■), as functions of Re. The dashed line is a linear plus quadratic fit to the Lyapunov data. The uncertainties in the measured quantities are estimated to be about 10%. The transition from periodic to weakly turbulent flow occurs around $Re = 35$ where the velocity fields separated by a forcing period begin to differ. All of these measures of mixing vary smoothly across the transition from periodic to weakly turbulent flow.

to each other and increase smoothly as a function of Re. These measures broadly characterize the stretching, transport, and ultimately the mixing properties of the system across the transition from periodic to non-periodic flow occurring near $Re = 35$. It is interesting that these quantities vary smoothly through the transition to non-periodic flow. The monotonically increasing trend for these various quantities is similar to the behavior of dye mixing rates determined previously [7]. In that work, the experimental dye mixing rates were about an order of magnitude less than what one would calculate for the rate predicted from the Lyapunov distribution [25]. For our measurements, we find that $\langle\lambda\rangle \approx \sigma_{rms}/3$ and that $\alpha \approx \langle\lambda\rangle/6$. This latter relationship suggests a similar decrease in mixing here owing to the time required to transport fluid across the cell [7], although a quantitative correspondence is difficult to establish.

Our measurements of stretching fields demonstrate quantitatively that, within the resolution of our data, several related measures of mixing are proportional and vary continuously through the transition between periodic and weakly turbulent flows. We also find that the scaled PDF of the Lyapunov exponent has a universal shape. These observations quantitatively demonstrate the application of material stretching concepts to weakly turbulent fluid states. The stretching field approach appears to hold significant promise for understanding mixing in other largely 2D flows, e.g., geophysical situations where rotation, stratification, or other sources of strong anisotropy single out a particular direction. Application of these ideas to fully 3D flows will require improved space and time resolution that is not yet obtainable experimentally.

We acknowledge useful discussions with D. Durian, G. Eyink and C. Connaughton. Work performed at Los Alamos National Laboratory was funded by the US Department of Energy under Contract No. DE-AC52-06NA25396.The work of JPG and PEA was supported by the NSF under Grant DMR-0405187.

[1] H. Aref, J. Fluid Mech. **143**, 1 (1984).
[2] J. M. Ottino, *The kinematics of mixing: stretching, chaos, and transport* (Cambridge University Press, Cambridge, UK, 1989), 1st ed.
[3] J. M. Ottino, Annu. Rev. Fluid Mech. **22**, 207 (1990).
[4] G. Haller and G. Yuan, Physica D **147**, 98 (2000).
[5] G. Haller, Phys. Fluids **14**, 1851 (2002).
[6] G. Voth, G. Haller, and J. P. Gollub, Phys. Rev. Lett. **14**, 254501 (2002).
[7] G. Voth, T. C. Saint, G. Dobler, and J. P. Gollub, Phys. Fluids **15**, 2560 (2003).
[8] F. Muzzio, P. Swanson, and J. Ottino, Phys. Fluids A **3**, 822 (1991).
[9] F. Varosi and T. M. Antonsen, Phys. Fluids A **3**, 1017 (1991).
[10] S. Shadden, F. Lekien, and J. E. Marsden, Physica D **212**, 271 (2005).
[11] M. Mathur, G. Haller, T. Peacock, J. Ruppert-Felsot, and H. L. Swinney, Phys. Rev. Lett. **98**, 144502 (2007).
[12] B. Shraiman and E. D. Siggia, Nature **405** (2000).
[13] D. R. Fereday, P. H. Haynes, A. Wonhas, and J. C. Vassilicos, Phys. Rev. E **65**, 035301 (2002).
[14] G. Falkovich, K. Gawedzki, and M. Vergassola, Rev. Mod. Phys. **73**, 913 (2001).
[15] M. C. Jullien, Phys. Fluids **15**, 2228 (2003).
[16] G. Boffetta and I. M. Sokolov, Phys. Fluids **14**, 3224 (2002).
[17] M. K. Rivera and R. E. Ecke, Phys. Rev. Lett. **95**, 194503 (2005).
[18] A. Pumir, B. I. Shraiman, and M. Chertkov, Phys. Rev. Lett. **85**, 5324 (2000).
[19] T. Burghelea, E. Segre, and V. Steinberg, Europhys. Lett. **68**, 529 (2004).
[20] B. Williams, D. Marteau, and J. P. Gollub, Phys. Fluids **9**, 2061 (1997).
[21] A. Wolf and H. Swinney, Physica D **16**, 285 (1984).
[22] J. Schneider, V. Fernandez, and E. Hernandez-Garcia, J. Marine Sys. **57**, 111 (2005).
[23] J. Schneider, T. Tel, and Z. Neufeld, Phys. Rev. E **66**, 066218 (2002).
[24] G. I. Taylor, Proc. Roy. Soc. A. **223**, 446 (1954).
[25] T. M. Antonsen, Z. Fan, E. Ott, and E. Garcia-Lopez, Phys. Fluids **11**, 3094 (1996).